Novel hydroxyapatite coating on new porous titanium and titanium-HDPE composite for hip implant

Xie, Jianhui; Luan, Ben Li; Wang, Jianfeng; Liu, Xing Yang; Rorabeck, Cecil; Bourne, Robert

Publisher's version / Version de l'éditeur:
https://doi.org/10.1016/j.surfcoat.2007.10.040
Surface & Coatings Technology, 202, 13, pp. 2960-2968, 2007-11-17

Novel Hydroxyapatite Coating on New Porous Titanium and Titanium-HDPE Composite for Hip Implant

Jianhui Xie, Ben Li Luan*, Jianfeng Wang, Xing Yang Liu

Integrated Manufacturing Technologies Institute

National Research Council

800 Collip Circle, London, Ontario Canada N6G 4X8

Cecil Rorabeck and Robert Bourne

London Health Science Center

339 Windermere Road, London, Ontario Canada N6A 5A5

* Corresponding author, email: ben.luan@nrc-cnrc.gc.ca, Phone: 519-430-7043

Abstract

Porous titanium (Ti) and Ti-high density polyethylene (Ti-HDPE) composite were investigated as new hip implant materials to increase the biomechanical compatibility by promoting a matching modulus of elasticity between hip stem and human bone. Surfaces of both materials were modified to increase its bioactivity and biocompatibility through electrochemical activation treatment and deposition of hydroxyapatite (HA) coating. The

electrochemical activation treatment of both materials in 10M NaOH solution creates a bone-like porous nanostructure across the surfaces, thus enhancing the growth of natural bone. A top layer with nanometer-pores and TiO_2 was formed during the activation process, creating a favorable and prerequisite condition conducive to the formation of hydroxyapatite coating. Furthermore, a layer of hydroxyapatite, a bioactive and biocompatible bioceramics that is the main component of natural bone, was deposited on the porous Ti and Ti-HDPE composite through a novel chemo-biomimetic method. The formed coating is characterized through TEM as a nanometer scale crystalline.

Key Words: Titanium, composite, hydroxyapatite, electrochemical activation, nanostructure.

1. Introduction

The attachment of metal prosthetic implants to adjacent bone continues to be a problem in orthopaedic surgery (1). Among the metallic materials for orthopaedic applications, titanium and titanium alloys are the most extensively investigated hip replacement materials. However, a critical challenge still exists in load-bearing implants, termed as "stress shielding" (2, 3). It is well known that bone regeneration and repair are promoted by mechanical loads (3-5). Titanium is much stiffer than bone (6), an implant of solid titanium therefore can carry a disproportionate amount of load. The surrounding bone is then stress-shielded and experiences abnormally low levels of stress, which can lead to resorption of bone and the consequent loosening of the implants (4, 5). Achieving a

matching stiffness through reduction the Young's modulus of the implant is therefore a crucial issue.

In order to achieve matching Young's modulus and improve long-term interface strength, efforts to develop porous metallic coating or porous bulk materials have been extensively conducted (7-11) to promote partial or complete bone anchoring and ingrowth, thus enhancing the strength of the interface and reducing the tissue encapsulation around the implants. The introduction of pores into structural material will dramatically change its mechanical properties, such as stiffness, strength and fatigue resistance. The anticipated reduction of the stiffness can be beneficial to reducing stress shielding, but the mechanical strength must be maintained.

One of the key issues for a durable and successful implant is a strong bone-implant interface. Surface properties such as wettability, chemical composition and topography, govern the biocompatibility of titanium. Surface roughness on the nanometer-scale has been shown to promote a reliable connection between bone and the implants and to reduce the fibrous tissue encapsulation (12). However, conventionally processed (e.g. cast, forged, etc) titanium currently used for orthopaedic and dental applications exhibits roughness only on a micrometer level but is smooth on a nanometer scale (13). New approaches were therefore attempted to design the next-generation of implants focusing on creating unique nanometer-topography (or roughness) on the implant surface, simulating the nanostructures such as collagen and hydroxyapatite in natural bone. One method to promote the long term interface strength is to develop apatite-type coating to

facilitate the osteo-conductivity, thus enhancing the complete anchoring and ingrwoth of natural bone onto the implants using different coating techniques (14-19). Much attention has focused on ceramics which resemble the mineral phase in bone tissues, i.e. hydroxyapatite (20-23).

This study presents a new approach for biomaterial application through a combination of reducing stress-shielding of implant materials using porous metals and promoting bone ingrowth into implant materials using porous and bioactive hydroxyapatite coating. In this investigation, a porous Ti and a Ti-HDPE composite were adopted as the implant materials. A nanometer roughness was created on top of the micro-roughness through an electrochemical activation treatment, followed by the deposition of hydroxyapatite to enhance the bioactivity and biocompatibility.

2. Experimental Details

2.1 Samples Preparation

Porous Ti and Ti-HDPE disks (about φ7.0mm×6 mm) were used for the coating experiments. The disks were fabricated by a powder compaction and sintering process. In the fabrication process, commercially pure (CP)-Ti powders (Fig. 1) (AEE, USA) were loaded into a case-hardened steel mold and uniaxially pressed into disks at a pressure of 105MPa. The green Ti disks were then loaded into a FP30 Vacuum Sintering Furnace

(Thermal Technology Inc., USA) and sintered under inert gas of helium at 1000°C for one hour. The resulted porosity of the sintered samples was about 33%. The Ti-HDPE composite was fabricated by infiltrating HDPE at elevated temperature into porous Ti disks. This process was conducted in a custom-made mold, in which HDPE powders (Exonmobil Chemical, USA) were loaded and melted, and the molten HDPE was infiltrated into the pores of the Ti disks at 200°C under a pressure of 2000psi.

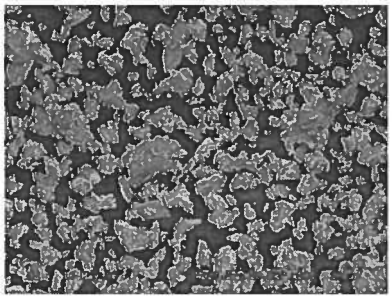

Fig.1 SEM micrograph of the CP-Ti powders

The disk specimens were mechanically polished using SiC paper #400 and #600, and 9μm Al_2O_3 paper. A titanium wire was welded to the disk for electrical conductivity and further handling. The polished samples were ultrasonically cleaned in acetone, ethanol and deionized water for 10 minutes, sequentially. The clean specimens were etched in a 0.2 *vol.* % HF (Caledon, 48%) + 0.4 *vol.* % HNO_3 (Fisher, 68-71%) solution for 10 minutes, rinsed thoroughly with deionized water, and subjected to ultrasonic cleaning for 10 minutes in deionized water and then dried at room temperature. The specimens were ready for further electrochemical activation treatment.

2.2 Electrochemical Activation Treatment

The electrochemical activation treatment, a prerequisite for the hydroxyapatite coating formation, was carried out using a HP E3610A DC power supply at room temperature in a 10M NaOH solution for 45 minutes. A potentiostatic voltage of 10V was applied between a Ti disk as anode (about φ7.0mm×6 mm) and two Ti6Al4V plates (30×30mm^2) as cathodes.

2.3 Apatite Formation on the Activated Specimens

The apatite coating was formed in a solution with enhanced Ca^{2+} and HPO_4^{2-} concentrations by a factor of five, 5(Ca&P), shown in Table 1, as compared to the conventionally used simulated body fluid (SBF) and blood plasma. The chemicals used for the solution are reagent grade, including NaCl (Fluka, ≥99.5%), $NaHCO_3$ (Sigma-Aldrich, ≥99.7%), KCl (Fisher, ≥99.6%), Na_2HPO_4 (Sigma-Aldrich, >99.0%), $MgCl_2.6H_2O$ (Sigma-Aldrich, >99.0%), $CaCl_2.6H_2O$ (Fisher, ≥99.5%), Na_2SO_4 (Anachemia, >99.0%).

Table 1 Chemical composition (mM) of SBF, blood plasma and 5(Ca&P) solution

	Na^+	K^+	Mg^{2+}	Ca^{2+}	Cl^-	HCO_3^-	HPO_4^{2-}	SO_4^{2-}
5(Ca&P)	142.0	5.0	1.5	12.5	159.0	4.2	5.0	0.5
Blood plasma	142.0	5.0	1.5	2.5	103.0	27.0	1.0	0.5
SBF	142.0	5.0	1.5	2.5	148.8	4.2	1.0	0.5

The apatite formation in the 5(Ca&P) solution was conducted in beakers using a chemo-biomimetic method (24). The novel approach presented in this communication is termed "chemo-biomimetic HA coating process" for two reasons: 1) the deposition is based on the conventional biomimetic process simulating the natural bone growth, and 2) chemical modifications were conducted with respect to the substrate surface chemistry and topographic features prior to HA deposition as well as to the composition of deposition solutions, more specifically, increased calcium and phosphate concentrations. Both modifications were designed to accelerate the deposition process. The solution was buffered at pH of 6.50 with its temperature maintained at 37°C in a water bath.

2.4 Characterization of the Activated Ti substrates and Hydroxyapatite Coating

X-ray photoelectron spectroscopy (XPS) is a very surface sensitive analytical technique that provides elemental and chemical state data from the outer 5-10 nm of a surface. XPS was carried out with a Kratos AXIS Ultra spectrometer using a monochromatic Al Kα source (20mA, 14kV). The instrument was calibrated to give a binding energy (BE) of 83.96eV for the Au $4f_{7/2}$ line for metallic gold and the spectrometer dispersion was adjusted to give a BE of 932.62eV for the Cu $2p_{3/2}$ line of metallic copper. The Kratos charge neutralizer system was used on all specimens. Survey spectra was collected with a pass-energy of 160eV and an analysis area of ~300×700 μm^2. High-resolution spectra was obtained using a 20eV pass-energy and an analysis area of ~300×700 μm^2. All high-

resolution spectra were charged reference to adventitious carbon at 285.0eV. Spectra were analyzed using CasaXPS software (version 2.2.19) (Fairley Inc, 1999-2003).

Nanometer-scale porous surface morphologies of the activated porous Ti and Ti-HDPE composite were observed using Hitachi S-4500 field emission SEM (FESEM) equipped with an EDAXTM EDX system. At high electron beam voltages (>15 kV) a spatial resolution of <2 nm is attainable.

The observation of surface morphologies of the deposited hydroxyapatite coating was conducted using Hitachi S-3500N SEM/EDX with a practical spatial resolution of 100nm. The nanometer grain size of formed hydroxyapatite coating was characterized using Philips CM20 Transmission Electron Microscope (TEM). The coating was scratched off the substrates, dispensed in Ethanol, attached on a copper screen mesh for TEM analysis.

3. Results and Discussions

3.1 Surface Nanostructure of the Activated Porous Ti and Ti-HDPE Composite

The microstructures of the porous Ti and the Ti-HDPE composite are shown in Fig. 2. The necking between titanium particles due to sintering process creates an open network of pores on the porous Ti disk. The HDPE polymer penetrates the entire cross section of

the disk and fills up the pores in the substrate (Fig. 2b). The infiltrated polymer interconnects within the pores, strengthening the porous Ti substrate. The polymer infiltration creates a solid composite with a metal substrate and a polymer network, leading to a reduced modulus of elasticity and a strengthened porous Ti framework.

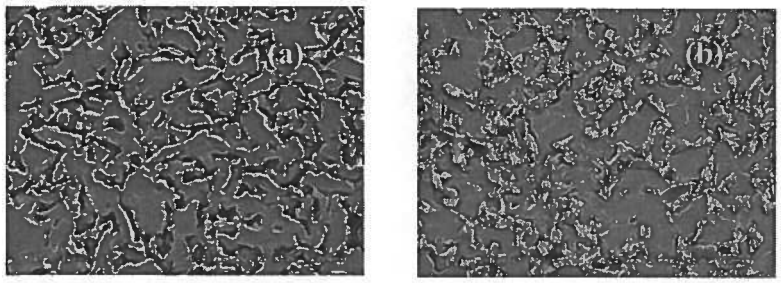

Fig. 2 SEM morphologies of (a) a porous Ti substrate and (b) a Ti-HDPE composite.

Bonding strength is an important factor in a successful implantation of artificial joints. Bare titanium alloy creates encapsulation of soft issues between bone and artificial joints, which prevents or hinders bone ingrowth. The surface of the titanium alloy for artificial joint should therefore be bioactive with favorable topographic features for the anchoring and ingrowth of bone. The electrochemical activation of the substrates creates a top layer of nanometer porous structure and TiO_2, a prerequisite condition for the deposition of hydroxyapatite coating. In addition to the nanometer-scale roughness with bioactive TiO_2 on top, a layer of bioactive hydroxyapatite coating on such features will further enhance the bone ingrowth.

Fig. 3 shows the surface nanostructure of electrochemically activated porous Ti substrate. Ridges formed during acid etching are still present, and a porous surface structure is present along the ridges (Fig. 3a). The surface porous structure is characterized of a network of circular nanometer pores of less than 200nm in diameter (Fig. 3b).

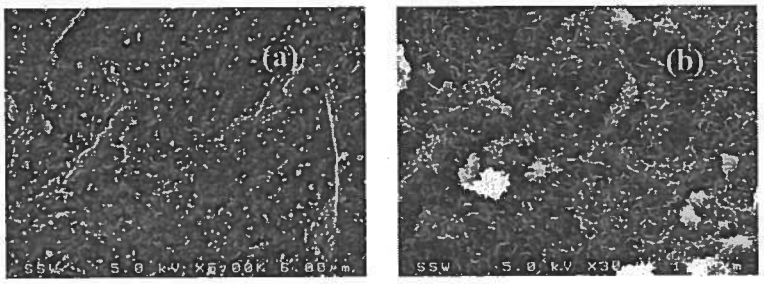

Fig. 3 FESEM micrographs of (a) the porous surface and (b) the network of surface nanometer pores on the electrochemically activated porous Ti substrate

For the Ti-HDPE composite after the electrochemical activation treatment, the ridges formed from the acid etching are also present on the surface. A wrinkled feature is shown across the surface (Fig. 4a). A nanometer scale pore structure is evenly distributed across the surface with a diameter of less than 100nm (Fig. 4b). The light colored area in Fig. 4c represents the infiltrated polymer.

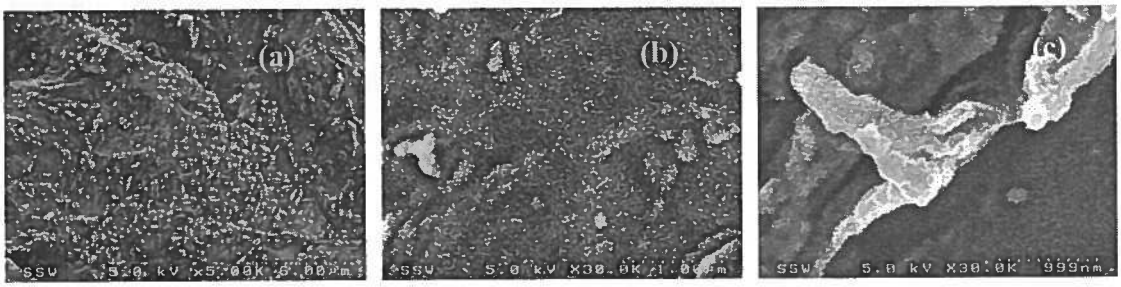

Fig. 4 FESEM micrographs of (a) ridges formed from the acid etching and the wrinkled surface, (b) the nanometer porous structure on the surface and (c) the activated HDPE polymers on the surface of electrochemically activated Ti-HDPE composite

Comparing the porous surface structure present on both substrates, the formed pores in the Ti-HDPE composite are much smaller and more uniform than those in the porous Ti substrate. This nanometer porous surface structure mimics the porous structure of natural bone. When these structured materials are implanted, the natural bone can readily grow into the pores and a strong bonding between the bone and the implants is therefore expected.

Another purpose of the electrochemical activation treatment is to create titanium oxide on the surface to promote the initiation of hydroxyapatite deposition through the reaction between Ca^{2+} and TiO_2 (6, 17). The XPS analysis shows that the Ti surface is completely converted to TiO_2 during activation (Fig. 5c). The Ar^+ sputter-cleaned Ti specimen (Fig. 5a) shows two peaks at the binding energies of 460.0eV and 453.9eV, attributable to Ti 2p1/2 and Ti 2p3/2 peaks, respectively. The acid-etched specimen (Fig. 5b), which were air-exposed, shows the most dominant peak at ~459eV, a second dominant peak at ~465eV, and a small third peak at ~454eV. The first two dominant peaks are mostly attributed to oxidized titanium with a minor contribution of Ti metal 2p1/2 at 460.1eV. The small third peak at 453.9eV is attributed to Ti metal 2p3/2. Since the formed oxide is very thin (less than 5-10 nm in thickness), the Ti metal peaks are still shown in the

spectrum, while the Ti metal 2p3/2 peak decreases significantly as oxide is formed on the specimen surface. High resolution XPS spectrum of Ti 2p peaks for the electrochemically activated specimen (Fig. 5c) show that Ti 2p is no longer present, suggesting the formation of a thicker oxide layer on the surface (>5-10 nm). Both Ti 2p peaks correspond to Ti^{4+} valence state, indicating the absence of sub-oxides such as TiO, Ti_2O_3 or Ti_3O_5. The O 1s peaks (Fig. 5d) are fitted with three different components, lattice oxide (O^{2-}), hydroxide (physisorbed -OH), and water (chemisorbed H_2O). There is a major peak at 530.5 ± 0.3 eV attributed to lattice oxide and minor O 1s peaks at higher binding energies attributable to hydroxides (532.0 eV) and chemisorbed H_2O (533.2 eV). During the electrochemical activation, the oxide layer thickens predominantly with the lattice oxide.

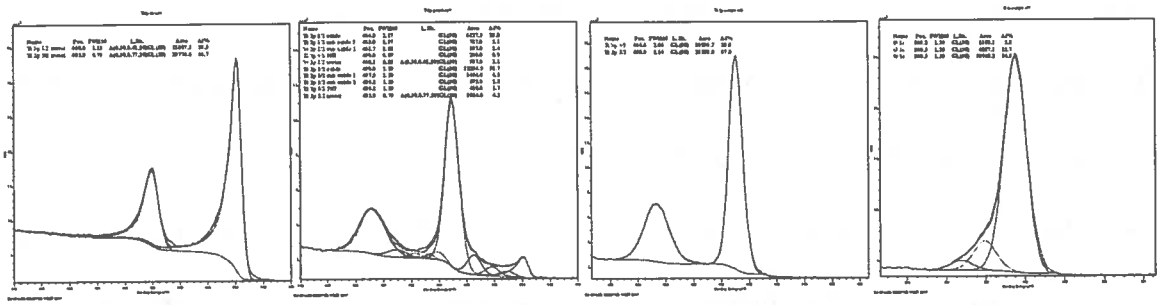

(a) (b) (c) (d)

Fig. 5 Ti 2p high resolution XPS spectrum for (a) Ar^+ sputtered, (b) acid etched and (c) electrochemically activated Ti alloys; O1s high resolution XPS spectrum for (d) electrochemically activated titanium Ti alloy

During the electrochemical activation process in the alkaline solution, the naturally formed thin titanium oxide is easily dissolved due to the reaction with OH^- to form $HTiO3^-$. The subsequently exposed Ti is electrochemically oxidized in the alkaline solution possibly according to the following reaction (1):

$$Ti(s) + 3OH^-(aq.) - 3e \rightarrow TiO_2.H_2O(s) + \frac{1}{2}H_2(g) \qquad (1)$$

Gas evolution was observed on the Ti substrates, possibly the result of hydrogen formation during the activation process. The XPS analysis shows that the oxidized Ti is in the Ti^{4+} valence state and the O is mainly in the form of lattice oxide (O^{2-}) with small amount of hydroxide (physisorbed OH^-) and water (chemisorbed H_2O), thus the surface of activated substrate is dominated by hydrated TiO_2 and possibly Ti-OH^- hydrogel layer.

3.2 Formation of Hydroxyapatite Coating on Porous Ti and Ti-HDPE Composite

The porous nanostructures present on the surface of porous Ti and Ti-HDPE composite mimic the structure of natural bone. The nanometer-scale pores formed during activation process may also demonstrate a capillary effect, which absorbs and retains the NaOH solution in the pores, resulting in a higher local pH on the surface. In addition to the bioactive TiO_2, the alkaline environment on the surface from both the capillary effect and the Ti-OH^- layer is conducive to the heterogeneous nucleation of hydroxyapatite, according to the following reaction (2):

$$10Ca^{2+}(aq.) + 6PO_4^{3-}(aq.) + 2OH^-(aq.) \rightarrow Ca_{10}(PO_4)_6(OH)_2(s) \quad (2)$$

One of the main characteristics of metal oxides in aqueous solution is their point of zero charge (PZC), which represents the pH value of aqueous solution at which an immersed oxide surface has zero net charge. If the solution pH is greater than the pH at PZC of the metal oxide, the metal oxide is negatively charged, and vice versa. The charged surface and surrounding solution form a thin double layer, to which oppositely charged ions are attracted and initial reaction starts between the charged metal oxide and the attracted ions. The PZC of the TiO_2 was reported to be in the range of 5.5 to 6.0 (25). Accordingly, a negatively charged surface is expectable in the coating solution with a pH of 6.50 in this investigation. As such, the positively charged Ca^{2+} is attracted to the surface of Ti alloy and reacts with the TiO_2 to form $CaTiO_3$, the PZC of which was reported of 8.1 (26), causing the $CaTiO_3$–covered surface to be positively charged and the PO_4^{3-} attracted to the surface to participate in further reactions, leading to the formation of calcium phosphate.

With the formation of calcium phosphate apatite on the surface, the super-saturation of simulated physiological solution may promote preferential nucleation of apatite on the already-formed apatite than in the solution, because there is higher activation energy of the homogeneous nucleation of apatite in the simulated body fluid than on the apatite-covered surface. Thus further formation of the apatite coating continues preferentially on the initial apatite layer by spontaneous growth consuming calcium and phosphate ions from the surrounding simulated body fluid. A theoretical analysis (27) also indicated that

formation of hydroxyapatite exhibits a higher thermodynamic preference than that of octacalcium phosphate (OCP) and dicalcium phosphate (DCP), therefore the further formation of the coating proceeds in the form of hydroxyapatite, rather than OCP or DCP. Through the chemo-biomimetic method, hydroxyapatite coating was deposited on the porous Ti and Ti-HDPE composite substrates.

Hydroxyapatite coating is evenly deposited on the whole surface of Ti-HDPE composite disks (the two disks on the left in Fig. 6). On the contrary, even though there is much more hydroxyapatite coating formed on the surface of the porous Ti, the surface is not fully covered and the coating is not even (the two disks on the right in Fig. 6). This is possibly due to the difficulties in the lateral growth of HA across the pores.

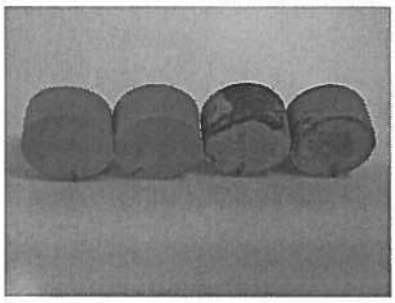

Fig. 6 Hydroxyapatite coating on the porous Ti (the two disks on the right) and Ti-HDPE composite (the two disks on the left)

3.2.1 Hydroxyapatite Coating on Porous Ti Substrate

Hydroxyapatite deposition initiates as spherical seeds at favorable sites on the surface. The spherical seeds grow as the deposition proceeds, gradually expand (as shown in Fig. 7a) and coalesce with adjacent seeds to form larger features (Fig. 7b) to eventually form a layer of hyhdroxyapatite coating (Fig. 7c). The initially formed hydroxyapatite is a porous bone-like structure with small pores, the final layer of hydroxyapatite still presents the spherical features and bone-like structure on the spheres. However, the surface of the porous Ti disk is not fully covered by hydroxyapatite coating, shown in Fig. 7a. Small islands of apatite are situated on the uncovered surface, some of them are so tiny that they appear as white dots on the uncovered surface.

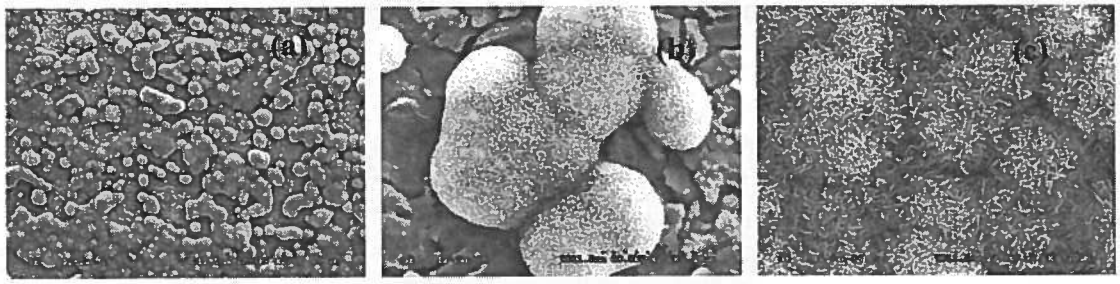

Fig. 7 SEM surface morphologies of (a) dispersed hydroxyapatite spheres, (b) an apatite island coalesced from expanding apatite spheres and (c) a layer of hydroxyapatite coating formed on the activated porous Ti substrate

The cross-section of the coated Ti disks was formed by breaking the samples mechanically to make a fresh fracture. The fracture surface of porous Ti shows randomly arranged Ti particles, and the particles are connected by necking areas (Fig. 8a). The curvature of the apatite spheres is clearly shown. With pores created from sintering on the

surface, the NaOH solution penetrates into substrate and the electrochemical activation treatment therefore modifies the inner surface of the pores, creating a favorable condition for the formation of hydroxyapatite coating to grow into the pores and encapsulate the Ti particles (Fig. 8b). It is also observed from the fractured apatite islands that the apatite spheres expand by layers.

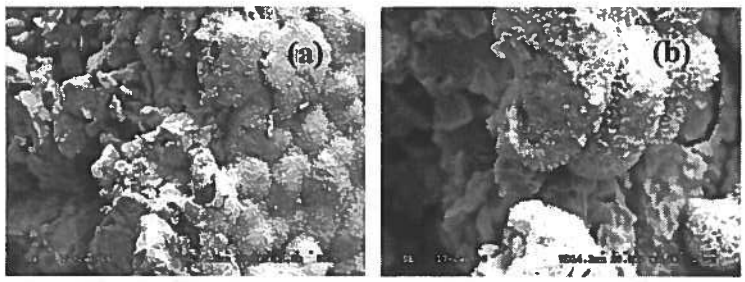

Fig. 8 SEM micrographs of (a) necking of Ti particles and the curvature of the hydroxyapatite spheres and (b) the expanding layers of the hydroxyapatite spheres on the cross-section of the fractured porous Ti substrate

3.2.2 Hydroxyapatite Coating on Ti-HDPE Composite

The hydroxyapatite coating can grow across the infiltrated polymer to evenly cover the surface of the Ti-HDPE composite (Fig. 9a), and the formed hydroxyapatite coating is intact even though the infiltrated polymer was pulled out (Fig. 9b), leaving a cavity underneath the hydroxyapatite coating.

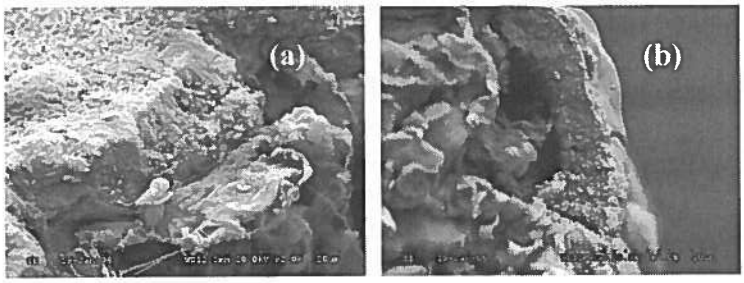

Fig. 9 SEM micrographs of (a) the hydroxyapatite coating on the HDPE polymer and (b) the intact hydroxyapatite coating across a pulled out polymer on the Ti-HDPE composite

The deposition and growth of hydroxyapatite coating on the Ti-HDPE composite (Fig. 10a) also follow similar patterns as is the case on the porous Ti substrate. The hydroxyapatite coating demonstrates spherical features on the surface and is characterized of bone-like porous microstructure (Fig. 10b). It appears that the coating is uniform and fully covers the surfaces, even though small voids are still present (Fig. 10c). Further analysis suggests that the uncovered area is related to the HDPE polymer. The fact that all the surrounding Ti substrate is covered by hydroxyapatite confirms that favorable condition for the formation of hydroxyapatite coating is only created on the Ti substrate, even though similar porous microstructure is observable on the polymer (Fig. 4c). In Summary, it appears that hydroxyapatite starts to deposit as spheres on the Ti substrate, and expands laterally across the polymer to form a uniform coating layer on the substrate surface as the deposition proceeds. This can be directly observed in Fig. 9 which shows the still intact HA coating on HDPE even after fracturing.

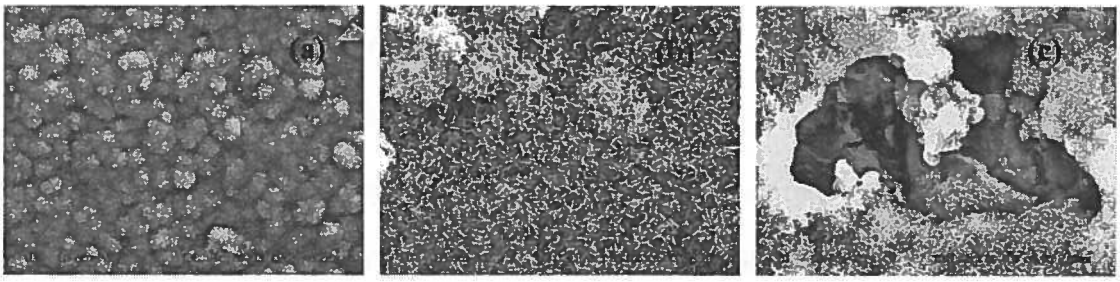

Fig. 10 SEM morphologies of (a) spherical structures and (b) the bone-like porous microstructure, and (c) the defects of the hydroxyapatite coating on the Ti-HDPE composite

Smaller nanometer pores on the surface of Ti-HDPE composite create more active sites for nucleation of hydroxyapatite deposition, and more nuclei indicate less required growth of individual seed to coalesce and form larger features to eventually cover the substrate surface. In addition to this favorable horizontal growth of coating, the thickening of HA is also benefited due to the more favorable thermodynamics of HA formation on the existing HA layer [28, 29]. In the case of the Ti-HDPE composite, the infiltrated polymer functions as a linkage of HA growth on the original titanium particles, resulting in an easier coverage on the surface. As for the porous Ti without the bridging polymer, the growth of hydroxyapatite needs to proceed along the curvature of the original titanium particles into the pores between the titanium particles. This growth gradually reduces the pore size and, at certain stage, results in concentration polarization inside such small cavities which prohibit further growth of HA. This is consistent with the observation, as shown in Fig. 7a.

TEM analysis (Fig. 11) shows that the nanometer-scale hydroxyapatite crystals were deposited on the surface of the activated titanium alloy with a grain size of less than 20nm (Fig. 11a). The micrograph of one single hydroxyapatite plate (Fig. 11b) also demonstrates that the grain of the formed hydroxyapatite is less than 30 nm in size. The formed nanocrystalline hydroxyapatite mimics the crystal structure of natural bone. The grain refinement to nanometer scale is expected to enhance the bioactivity and biocompatibility of the implant. The strength of the formed hydroxyapatite coating is also expected to increase with the grain refinement according to Hull-Patch equation, thereby reducing the wear of the implant surface.

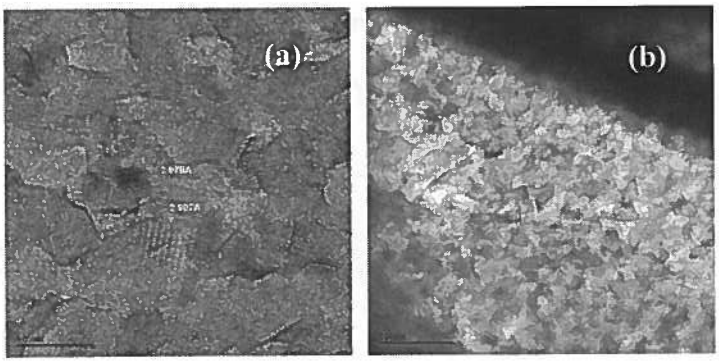

Fig. 11 TEM analysis of the formed hydroxyapatite coating, (a) nanometer grain size and (b) morphologies of a single hydroxyapatite plate, showing the nanometer grain size

4. Conclusions:

Electrochemical activation treatment in NaOH solution effectively creates nanometer bone-like porous structure on porous Ti and Ti-HDPE composite substrates. There are finer pores on the Ti-HDPE composite than on the porous Ti substrate. During activation, a bioactive TiO_2 layer is created on the substrate surfaces. This bioactive layer, combined with the nanometer-scale porous structure, establishes a favorable condition for the formation of hydroxyapatite deposit. As a result, hydroxyapatite coating is successfully deposited on the surface of both substrates through a chemo-biomimetic method. The deposit is more uniform with a higher coverage on the Ti-HDPE composite than on porous Ti, even though a greater amount of deposit is observed on the porous Ti substrate. Hydroxyapatite initially deposits on the activated surface as spherical features which expand and coalesce with neighboring features to gradually form a coating layer with porous bone-like surface structure. The formed hydroxyapatite coating is characterized as nanometer-scale crystalline with a grain size of less than 30nm.

This study clearly confirms the feasibility to concurrently enhance both the biochemical and the biomechanical compatibilities of existing Ti6Al4V hip implant. The favorable nanostructure created using the new activation and deposition processes is expected to promote bone ingrowth and enhance the interface strength.

Acknowledgements

This project is financially supported by CIHR-NRC Science and Technology Convergence Program for Innovation. The authors greatly appreciate Mr. D. Wang of NRC-ICPET for the TEM analysis and Mr. John Nagata for technical support.

References:

1. D. D. Nelson, H. E. Rubash and D. C. Mears, "Cartilage and bone ingrowth into porous titanium implants", Titanium Alloys in Surgical Implants. ASTM STP 796, H. A. Luckey and Fred Kubli, Jr., Eds., American Society for Testing and Materials, 1983, pp. 255-264.
2. Sarah, Francois Barthelat, L. Catherine Brinson, "Mechanical consideration for microporous titanium as an orthopedic implant material", Journal of Biomedical Materials Research, 69A:601-610, 2004.
3. J.J. Jacobs, D. R. Sumner, J. O. Galante, "Mechanism of bone loss associated with total hip replacement", Orthop. Clin. North Am. 24 (4): 583-590, 1993.
4. G. van Lenthe, M. waal Malefijt, R. Huiskes, "Stress shielding after total knee replacement may cause bone resorption uin the distal femur", J. Bone Joint Surg. Br., 79 (1): 117-122, 1997.
5. Z. N. Wan, L. D. Dorr, T. Woodstone, A. Ranawat and M. Song, " Effect of stem stiffness and bone stiffness on bone remodeling in cemented total hip replacement", J. Arthroplasty, 14 (2): 149-159,1999.

6. P. G. T. Geesink and M. T. Manly, Hydroxyapatite Coating in Orthopaedic Surgery, Raven Press, Ltd., New York, USA, 1993, p10.
7. P. Ducheyne, M. martens, P. de Meester and J. C. Mulier, "Titanium implants with porous structure for bone ingrowth: a general approach", Titanium Alloys in Surgical Implants. ASTM STP 796, H. A. Luckey and Fred Kubli, Jr., Eds., American Society for Testing and Materials, 1983, pp. 265-279.
8. Shigeru Nishiguchi, Hirofumi Kato, Masashi Neo, Masanori Oka, Hyun-Min Kim, Tadashi Kokubo and Takashi Nakamura, 'Alkali- and heat-treated porous titanium for orthopedic implants", Journal of Biomedical Materials Research, 54: 198-208, 2001.
9. Y. B. An, N. H. Oh, Y. W. Chun, Y. H. Kim, J. S. Park, etc. "Mechanical properties of environmental-electro-discharge-sintered porous Ti implants", Materials Letters 59: 2178-2183, 2005.
10. H. Q. Nguyen, D. A. Deporter, R. M. Pilliar, N. Valiquette, R. Yakubovich, "The effect of sol-gel-formed calcium phosphate coatings on bone ingrowth and osteoconductivity of porous-surfaced Ti alloy implants", Biomaterials, 25: 865-876, 2004.
11. I. H. Oh, N. Nomura and S. Hanada, "Microstructures and mechanical properties of porous titanium compacts prepared by powder sintering", Materials Transaction, 43 (3): 443-446, 2002.
12. Kim HM, Miyaji F, Kokubo T and Nakamura T. Preparation of bioactive Ti and its alloys via simple chemical surface treatment. J Biomed Mater Res 1996; 32: 409-417.

13. Yao C, Slamovich EB, Webster TJ. Titanium nanosurface modification by anodization for orthopedic application. In: Materials Research Society Symposium Proceedings. Nanoscale materials Science in Biology and Medicine. Boston, MA: Purdue Univ Lafayette IN; 2004, p215.

14. K. A. Khor, Y. W. Gu, D. Pan, P. Chang, "Micro structure and mechanical properties of plasma sprayed HA/YSZ/Ti-6Al-4V composite coatings", Biomaterials. 25 (18): 4009-4017, 2004

15. T. Kasuga, H. Kondo and M. Nogami, "Apatite formation on TiO_2 in Simulated body fluid", Journal of Crystal Grwoth, 235: 235-240, 2002.

16. J. M. Zhang, C. j. Lin, Z. D. Feng and Z. W. Tian, "Mechanistic studies of electrodeposition for bioceramic coatings of calcium phosphate by an in situ pH-microsensor technique", Journal of Electroanalytical Chemistry, 452: 235-240, 1998.

17. L. Jonášová, F. A. Müller, A. Helebrant, J. Strnad and P. Greil, "Biomimetic apatite formation on chemically treated titanium", Biomaterials, 25: 1187-1194, 2004.

18. A. Stoch, A. Brożek, G. Kmita, J. Stoch, W. Jastrzębski and A. Rakowska, "Electrophoretic coating of hydroxyapatite on titanium implants", Journal of Molecular Structure, 596: 191-200, 2001.

19. H. W. Kim, Y. H. Koh, L. H. Li, S. Lee and H. E. Kim, "Hydroxyapatite coating on titanium substrate with titania buffer layer processed by sol-gel method", Biomaterials, 25: 2533-2538, 2004.

20. D. M. Brunette, P. Tengvall, M. Textor and P. Thomsen, Titanium in Medicine, Springer-Verlag Berlin Heidelberg New York, USA, 2001.

21. T. Kokubo, "Apatite formation on surfaces of ceramics, metals and polymers in body environment", Acta Materialia, Vol. 46 (1998), pp. 2519-2527.

22. Y. Tang, Y. Liu, U. Sampathkumaran, M. Z. Hu, R. Wang and M. R. De Guire, "Particle growth and particle surface interaction of ceramic thin films", Solid State Ionics, Vol. 151 (2002), pp69-78.

23. F. Barrere, P. Layrolle, C. A. van Bliterswijk and K. de Groot, "Biomimetic calcium phosphate coatings on Ti6Al4V: A crystal growth study of octacalcium phosphate and inhibition by Mg^{2+} and HCO_3^-", Bone, Vol. 25, No.2 supplement, (1999), pp.107S-111S.

24. J. Xie and B. Luan, "Nanometer–scale surface modification of Ti6Al4V alloy for orthopedic applications", Journal of Biomedical Materials Research, Part A, 2007 (in press).

25. M. Kosmulski, "The pH-dependant surface charging and the points of zero charge", Journal of Collid and Interface Science, Vol. 253 (2002), pp 77-87.

26. T. hanawa, M. Kon, H. Doi, H. Ukai, K. Murakami, H. Hamanaka and K. Asaoka, "Amount of hydroxyal radical on calcium-ion-implanted titanium and point of zero charge of constituent oxide of the surface-modified layer", Journal of Materials Science: Materials in Medicine, Vol. 9 (1998), pp 89-92.

27. X. Lu, Y. Leng, "Theoretical analysis of calcium phosphate precipitation in the simulated body fluid", Biomaterials, Vol. 26 (2005), pp1097-1108.

28. Roger I. martin and Paul W. Brown, "Aqueous formation of hydroxyapatite", Journal of Biomedical Materials Research, Vol 35 (1997), pp299-308.

29. Wenju Wu, Hengzhong Zhuang and George H. nancollas, "Heterogeneous nucleation of calcium phosphates on solid surfaces in aqueous solution", Journal of Biomedical Materials Research, Vol 35 (1997), pp93-99.